Electronic Supplementary Material (ESI) for Physical Chemistry Chemical Physics.

Supplementary Information

Troponin structure: its modulation by Ca^{2+} and phosphorylation studied by molecular dynamics simulations

Juan Eiros Zamora[a], Maria Papadaki[b], Andrew E. Messer[b], Steven B. Marston[b] and Ian R. Gould[a]

[a]Department of Chemistry, Institute of Chemical Biology, Imperial College London, SW7 2AZ London, United Kingom
[b]National Heart & Lung Institute, Myocardial Function Section, Imperial College London, W12 0NN London, United Kingdom

Corresponding Author:
Ian R. Gould, PhD. Department of Chemistry, Imperial College London, SW7 2AZ London, United Kingdom. Email: i.gould@imperial.ac.uk

Table of Contents

Model primary sequence

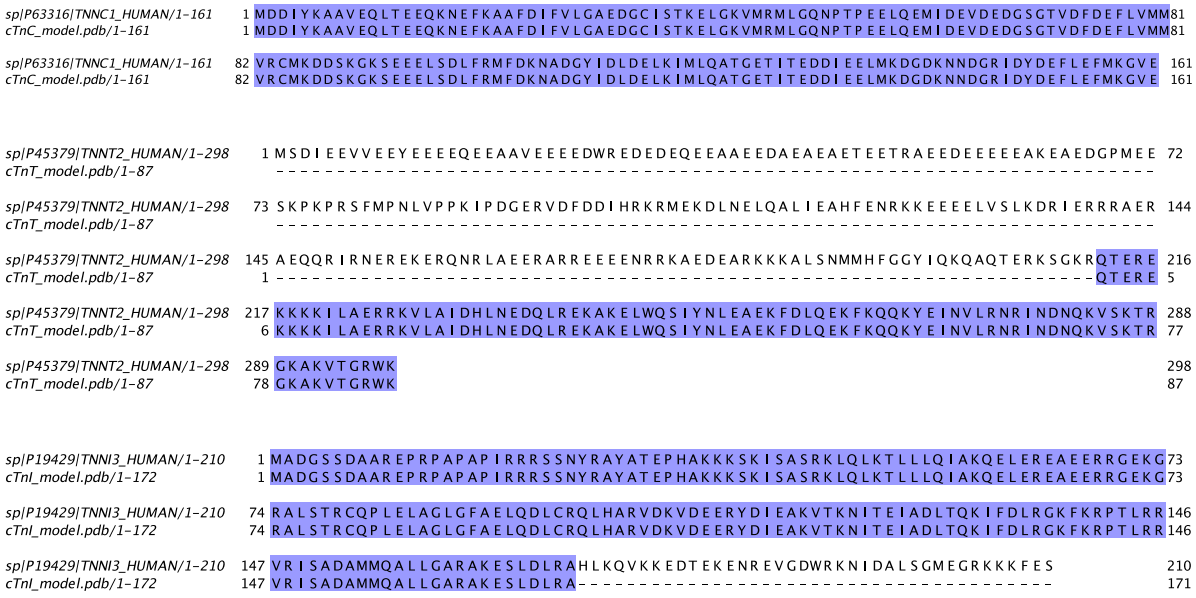

Figure S1. Sequence alignment of our cardiac Troponin model to the canonical human sequences of cTnC (top), cTnT (middle) and cTnI (bottom).

Root Mean Square Deviations

Wild Type cardiac Troponin

HMR refers to the MD trajectories obtained using the hydrogen mass repartition protocol, allowing for a time step of 4 fs. cMD refers to the trajectories obtained with a 2 fs timestep.

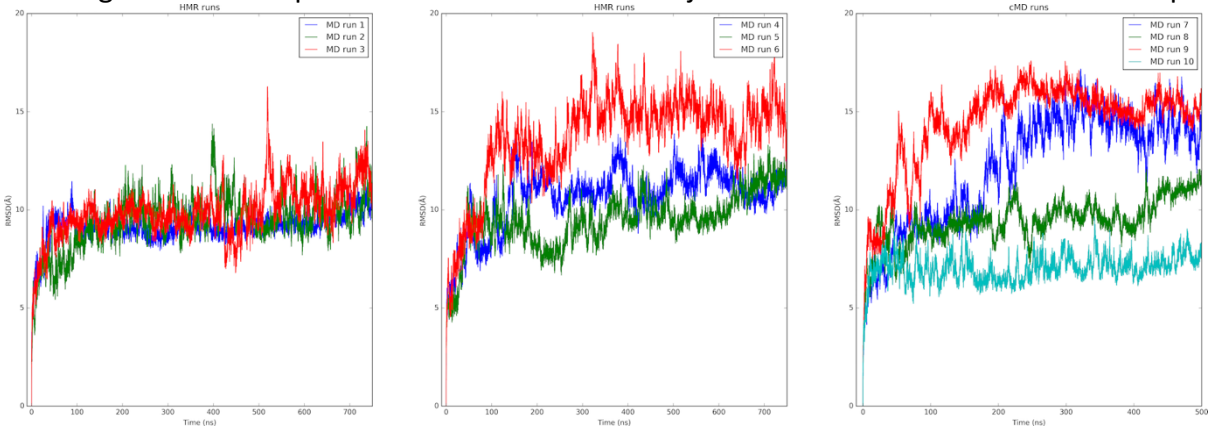

Figure S2. RMSD evolution through time for each individual WT trajectory. The RMSD is calculated for the backbone atoms against the first frame of each run.

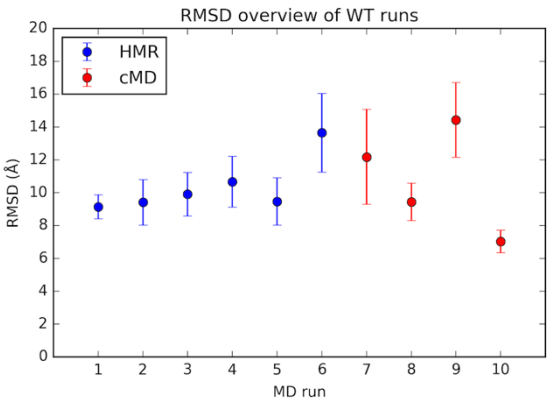

Figure S3. Summary of the RMSD results shown in Figure S2. Average RMSD values are plotted as dots and the standard deviation as error bars.

Table S1. Values used to generate Figure S3.

MD run	Average RMSD (Å)	Std. Dev. (Å)
1 (HMR)	9.14	0.72
2 (HMR)	9.41	1.38
3 (HMR)	9.91	1.32
4 (HMR)	10.66	1.55
5 (HMR)	9.45	1.44
6 (HMR)	13.65	2.40
7 (cMD)	12.18	2.89
8 (cMD)	9.44	1.13
9 (cMD)	14.43	2.27
10 (cMD)	7.04	0.69

RMSD analysis of the common regions of the model to the Takeda crystal structure, discarding the first 50 ns of simulation.

The residues in the model that match the crystal structure are presented in Table S2.

Table S2. Correspondence between the residues present both in our 419-residue cTn model and the PDB 1J1D (chains A to D) crystal structure.

Subunit	PDB 1J1D numbering	cTn model numbering
cTnC	1-89 (chain A)	1-89
cTnC	92-161 (chain A)	92-161
cTnT	202-271 (chain B)	162-231
cTnI	35-136 (chain C)	283-384
cTnI	145-160 (chain C)	393-408

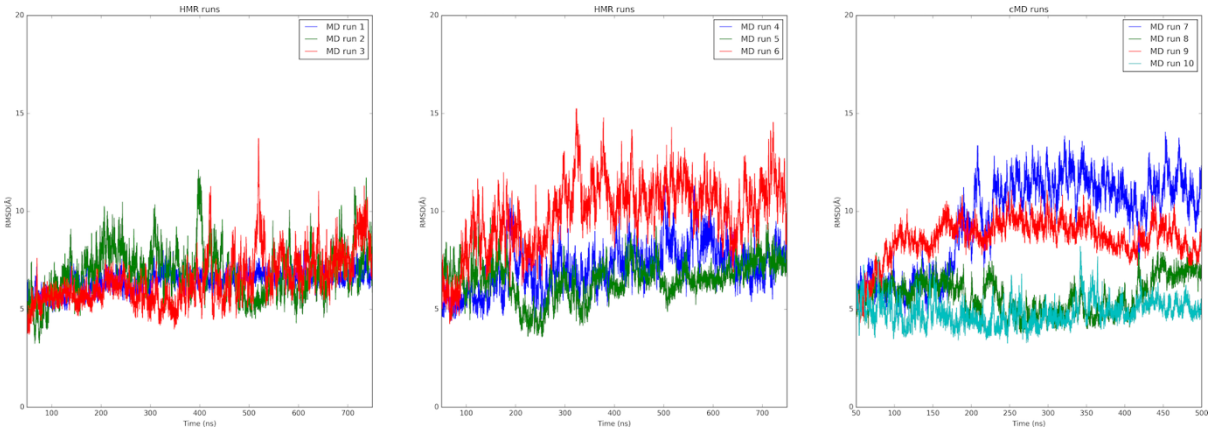

Figure S4. RMSD deviation of each run to the Takeda crystal structure (PDB 1J1D). The RMSD is calculated for the backbone atoms of the residues that are present in both structures. The first 50 ns of each simulation are discarded.

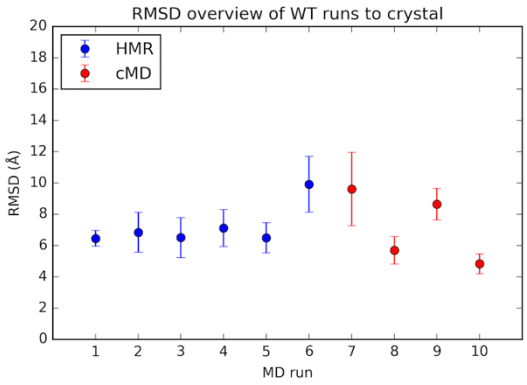

Figure S5. Summary of the RMSD results shown in Figure S4. Average RMSD values are plotted as dots and the standard deviations as error bars.

Table S3. Values used to generate Figure S5.

MD run	Average RMSD (Å)	Std. Dev. (Å)
1 (HMR)	6.46	0.51
2 (HMR)	6.85	1.27
3 (HMR)	6.51	1.28
4 (HMR)	7.12	1.18
5 (HMR)	6.50	0.96
6 (HMR)	9.91	1.78
7 (cMD)	9.61	2.35
8 (cMD)	5.70	0.89
9 (cMD)	8.65	1.02
10 (cMD)	4.83	0.63

Phosphorylated cardiac Troponin

S1P refers to the bis-phosphorylated systems that have each phosphoserine with a -1 chage, and SEP to each phosphoserine with a -2 charge.

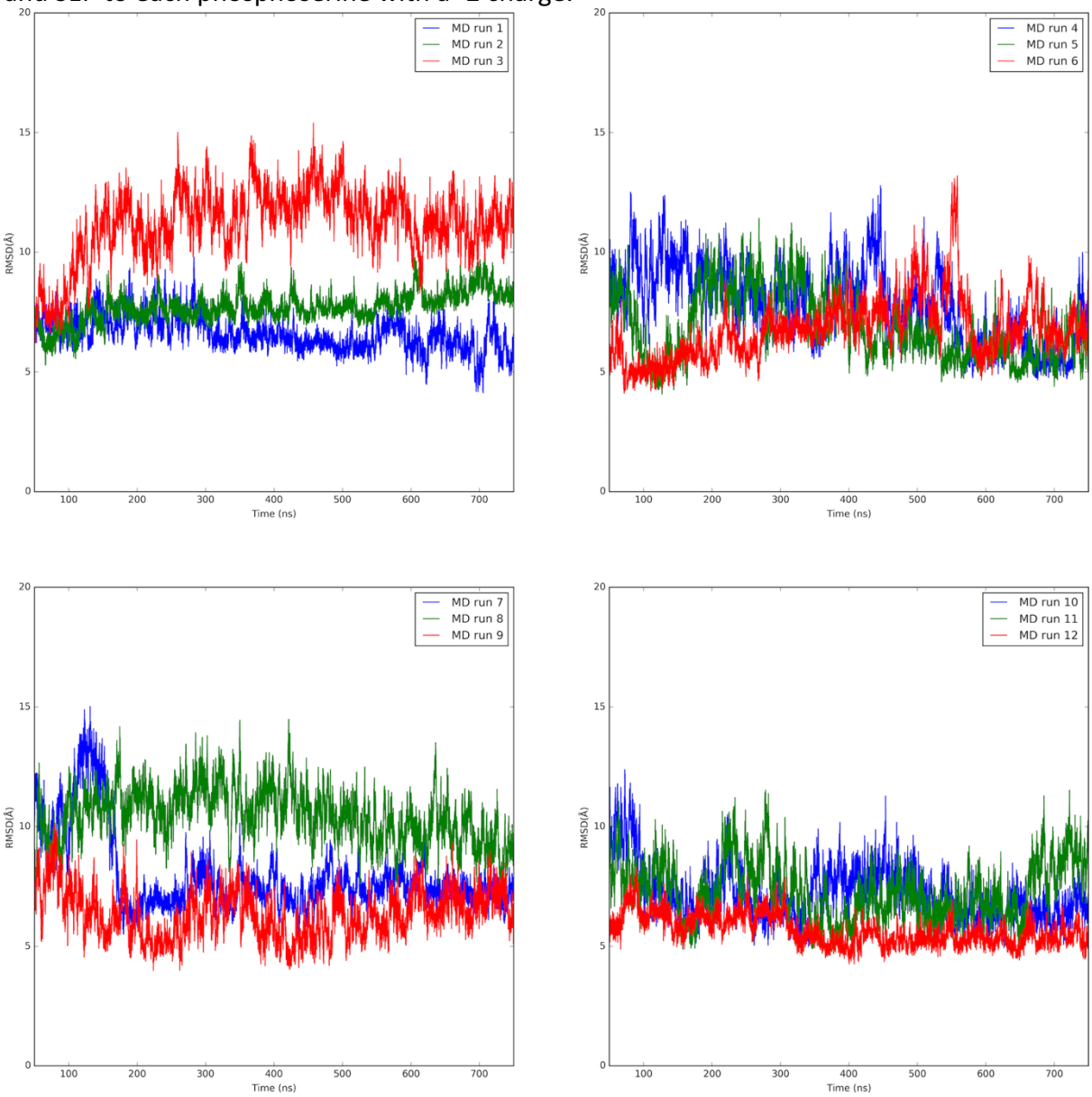

Figure S6. RMSD evolution through time for each individual SP23/SP24 trajectory to the Takeda crystal structure(PDB 1J1D). The RMSD is calculated for the backbone atoms of the residues that are present in both structures. The first 50 ns of each simulation are discarded.

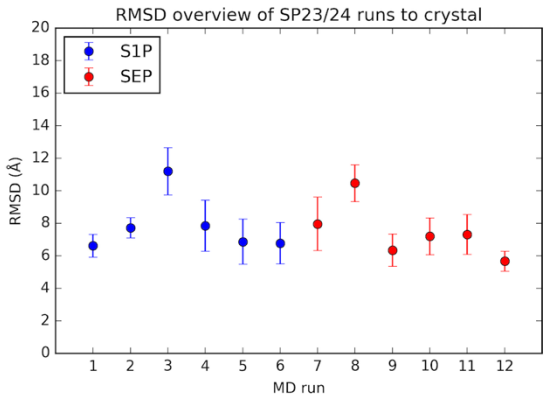

Figure S7. Summary of the RMSD results shown in Figure S6. Average RMSD values are plotted as dots and the standard deviations as error bars.

Table S4. Values used to generate Figure S7.

MD run	Average RMSD (Å)	Std. Dev. (Å)
1	6.61	0.7
2	7.72	0.63
3	11.2	1.46
4	7.85	1.57
5	6.87	1.38
6	6.77	1.27
7	7.96	1.65
8	10.46	1.12
9	6.34	0.99
10	7.2	1.13
11	7.31	1.22
12	5.67	0.62

First Principal Component motion representation

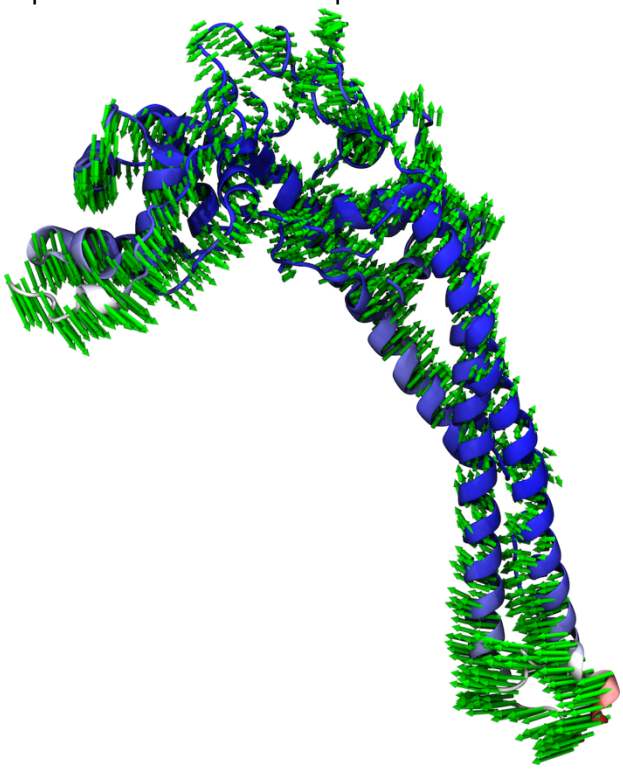

Figure S8. Hinge representation due to the contribution of each residue to the 1st Principal Component of motion. The backbone is colored from red to blue based on the specific contribution (blue being low and red high).

Clustering parameters

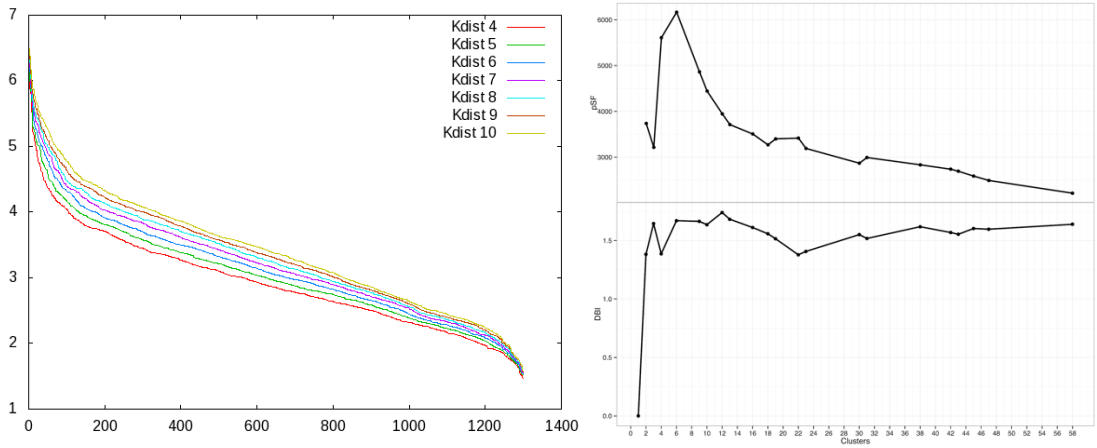

Figure S9. DBSCAN clustering parameters (left: sorted K-dist plot; right: pSF and DBI metrics) for the CcTnI region ($cTnI_{135-171}$) of the HMR WT runs. In this case, a cluster count of 4 is the best option.

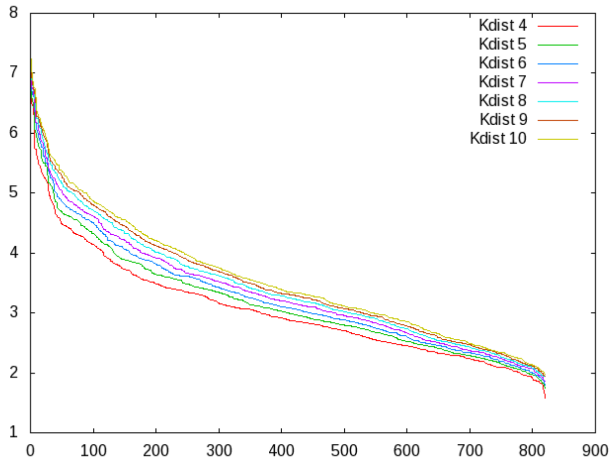
Kdist 4
Kdist 5
Kdist 6
Kdist 7
Kdist 8
Kdist 9
Kdist 10
1 2 3 4 5 6 7 8
0 100 200 300 400 500 600 700 800 900

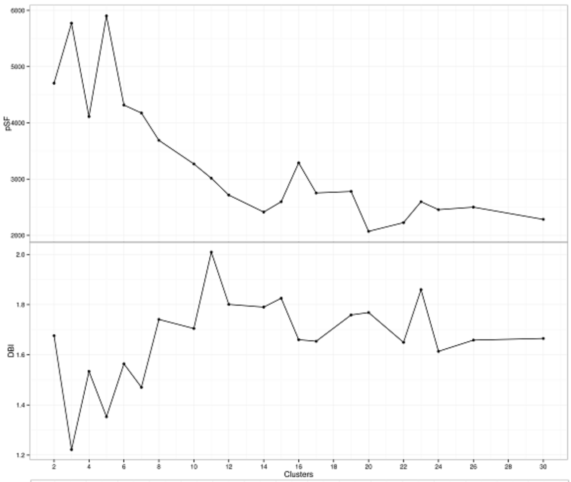
pSF
DBI
Clusters

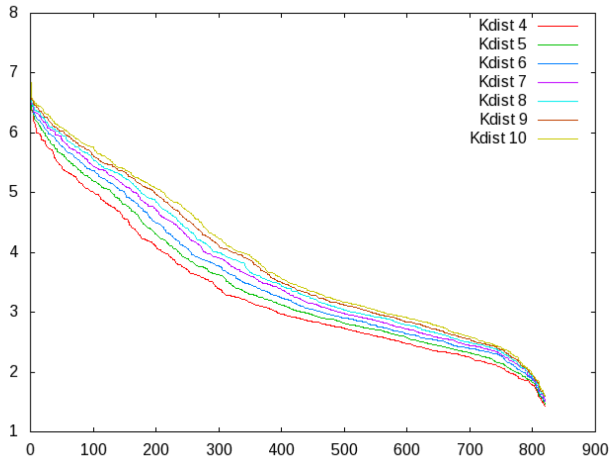
Kdist 4
Kdist 5
Kdist 6
Kdist 7
Kdist 8
Kdist 9
Kdist 10
1 2 3 4 5 6 7 8
0 100 200 300 400 500 600 700 800 900

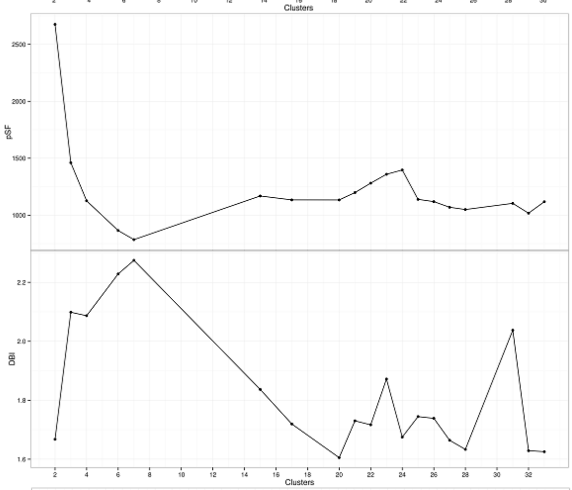
pSF
DBI
Clusters

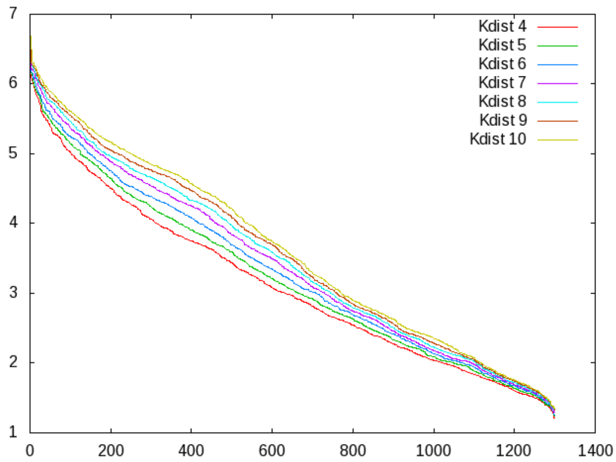
Kdist 4
Kdist 5
Kdist 6
Kdist 7
Kdist 8
Kdist 9
Kdist 10
1 2 3 4 5 6 7
0 200 400 600 800 1000 1200 1400

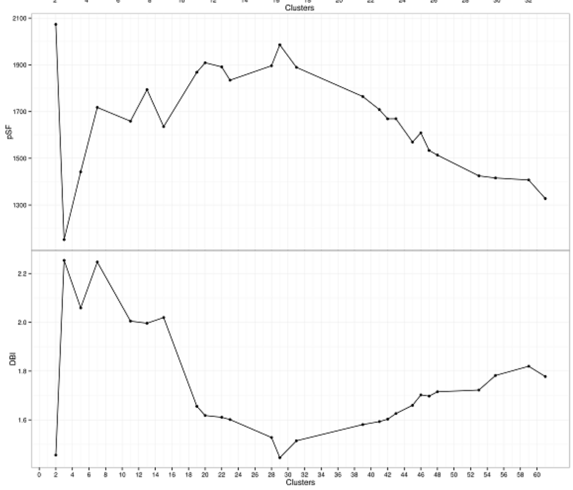
pSF
DBI
Clusters

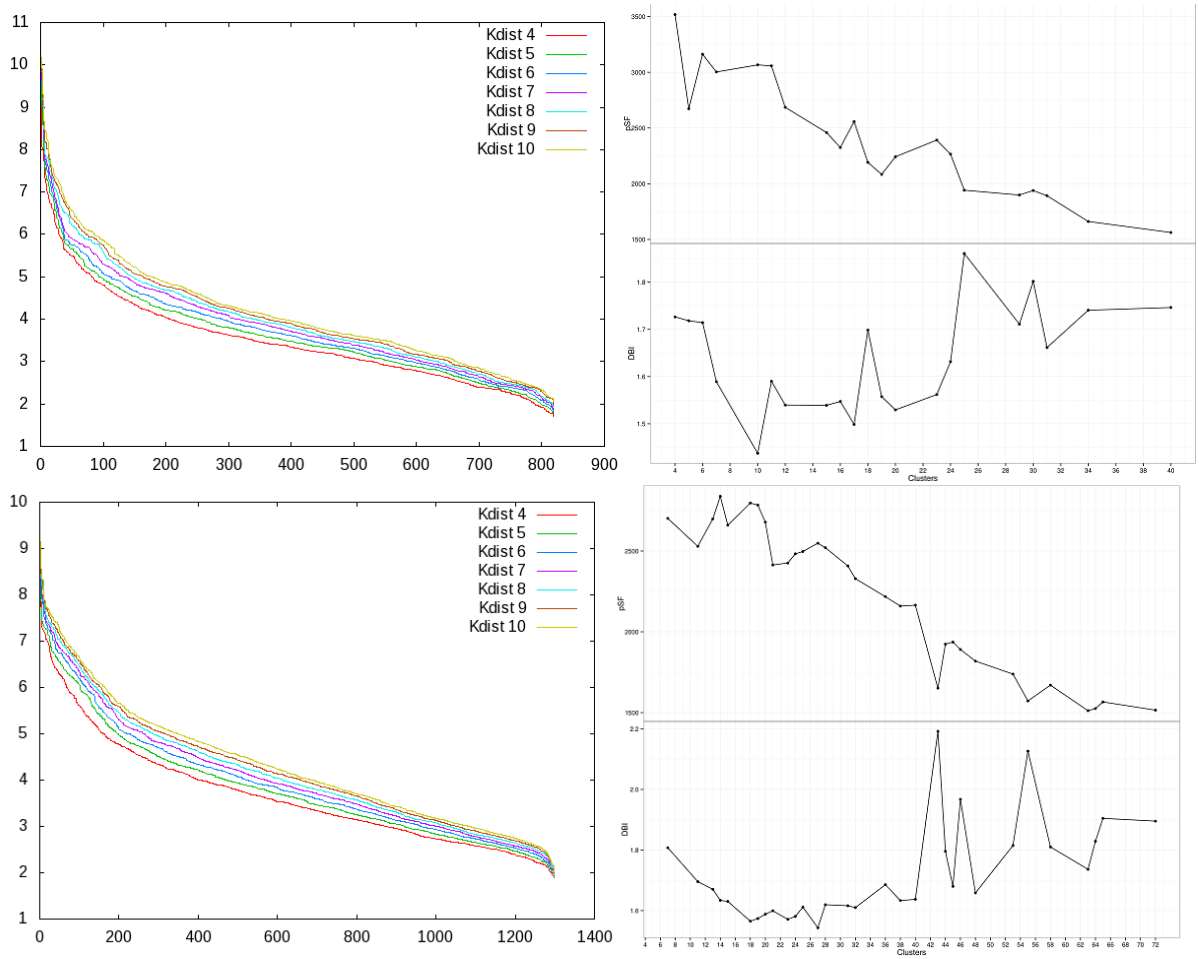

Figure S10. DBSCAN clustering parameters for the following regions and type of MD simulation, in order: CcTnI-cMD, CcTnT-cMD, CcTnT-HMR, NcTnI-cMD and NcTnI-HMR; where cMD corresponds to the WT simulations performed with a 2fs timestep and HMR to the ones using a 4fs timestep. The left graphs are the sorted K-dist plots, used to narrow down the area of ε and MinPnts parameters, and the right graphs are the pSF (top) and DBI (bottom) clustering metrics as a function of the cluster count, used to determine the optimal combination of ε and MinPnts.

Root Mean Square Fluctuations

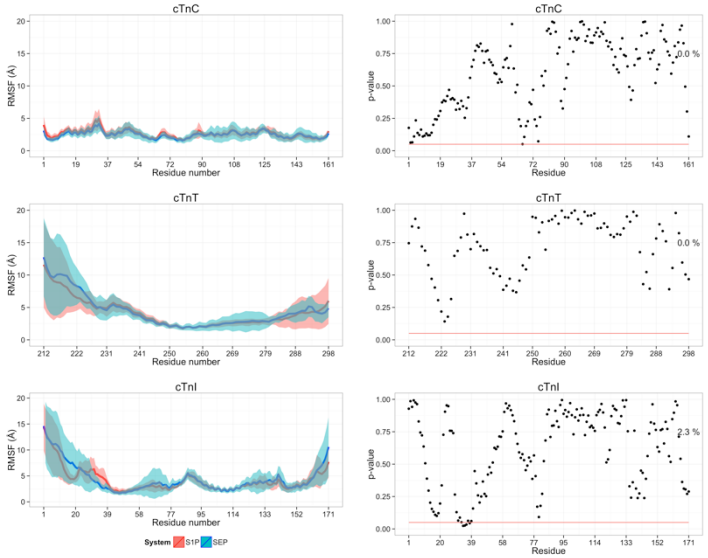

Figure S11. RSMF comparison between the two different types of SP23/SP24 systems that were simulated. S1P corresponds to both phosphoserines carrying a -1 net charge, and SEP to both carrying a -2 net charge (-2 and -4 total net charge on each system, respectively). As can be appreciated by direct comparison and from the T-test analysis, no significant difference in fluctuations can be distinguished between the two types of phosphorylation.

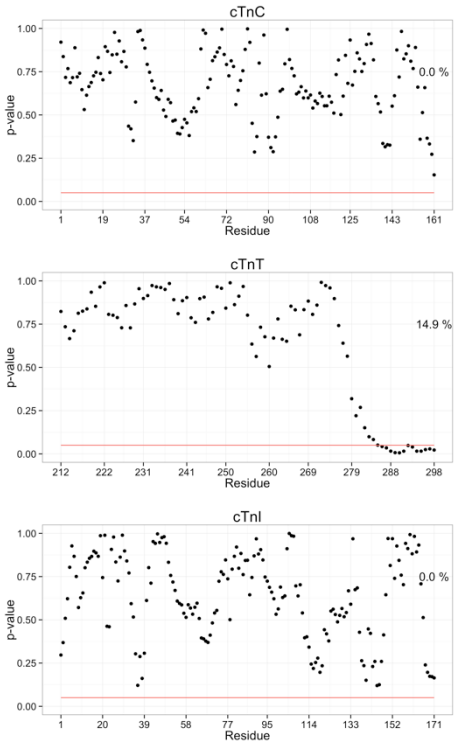

Figure S12. Results for the T-test between the RMSF values of the WT and SP23/SP24 systems. The Welch variant assuming varying variance and unequal sample size was used to calculate the 95% CI. Only the C-terminal cTnT region presents a significantly lower RMSF value after phosphorylation. As discussed in the main text, this could be an issue caused by the fact that the phosphorylated runs were started from the conformations obtained after the WT cluster analysis.

Catalytic Ca^{2+} coordination sphere distances

Time series

D65 OD1 and OD2

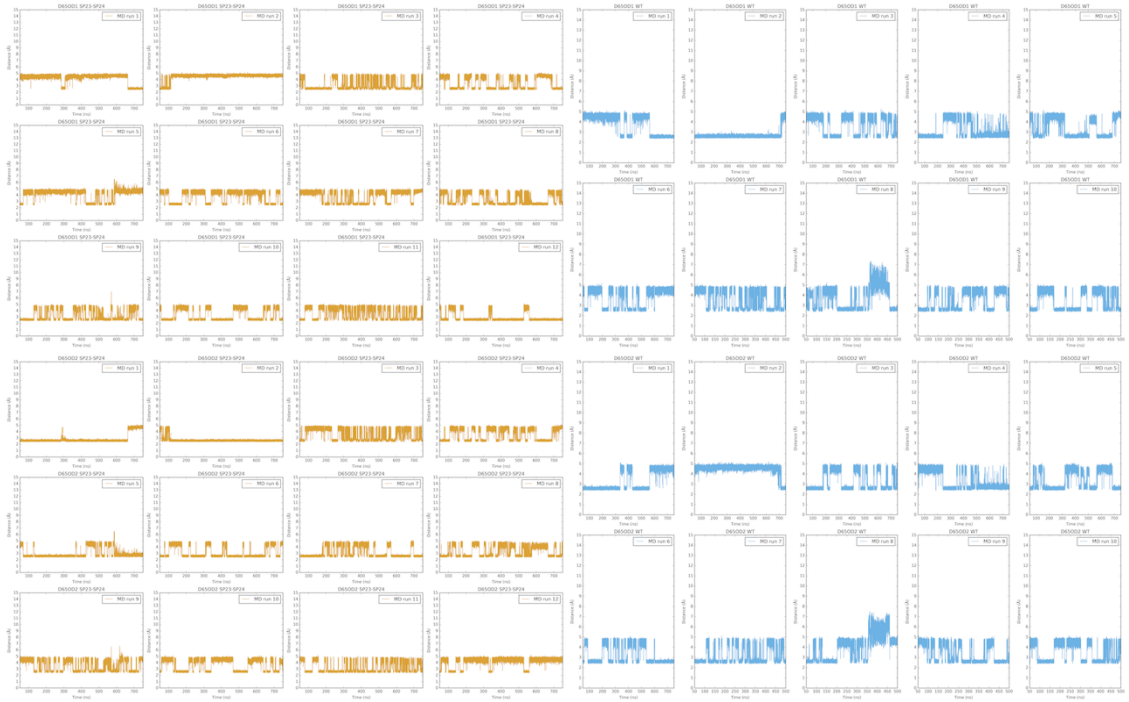

D67 OD1 and OD2

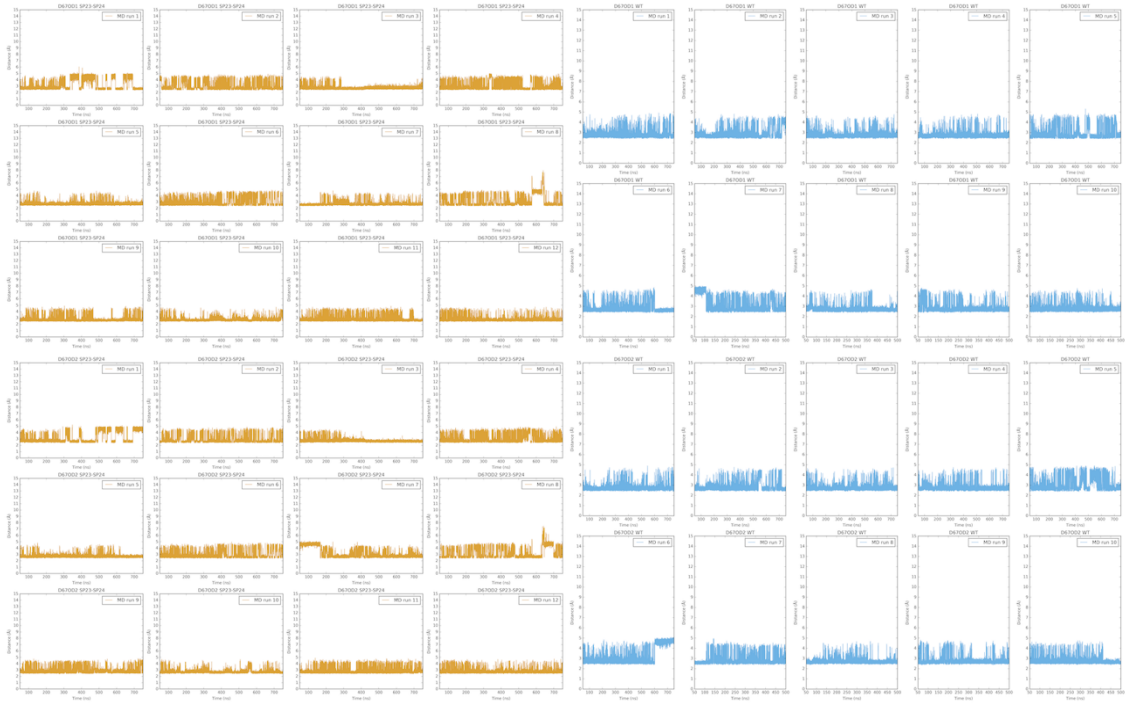

D73 OD1 and OD2

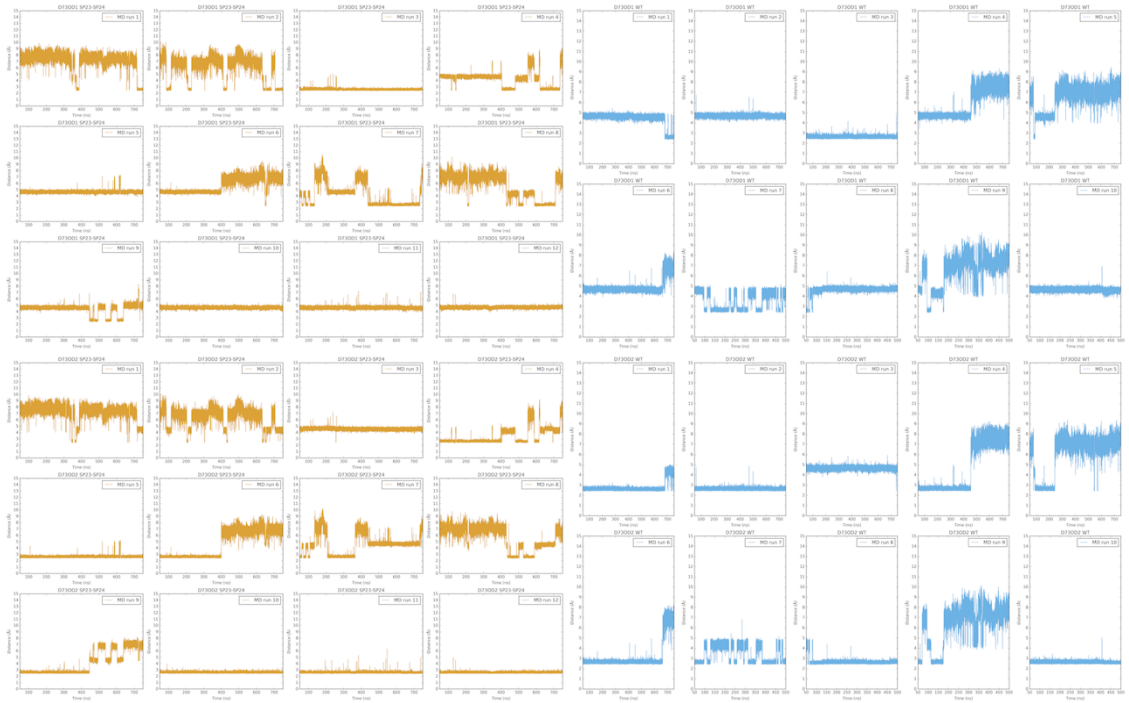

D75 OD1 and OD2

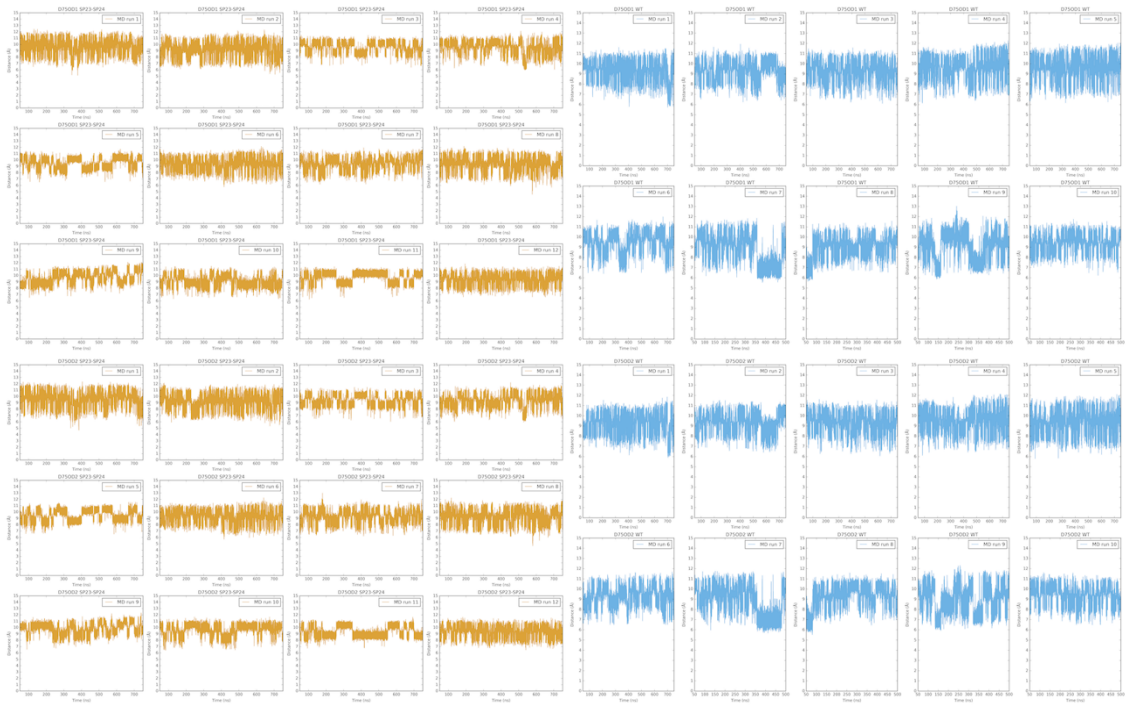

E66 OE1 and OE2

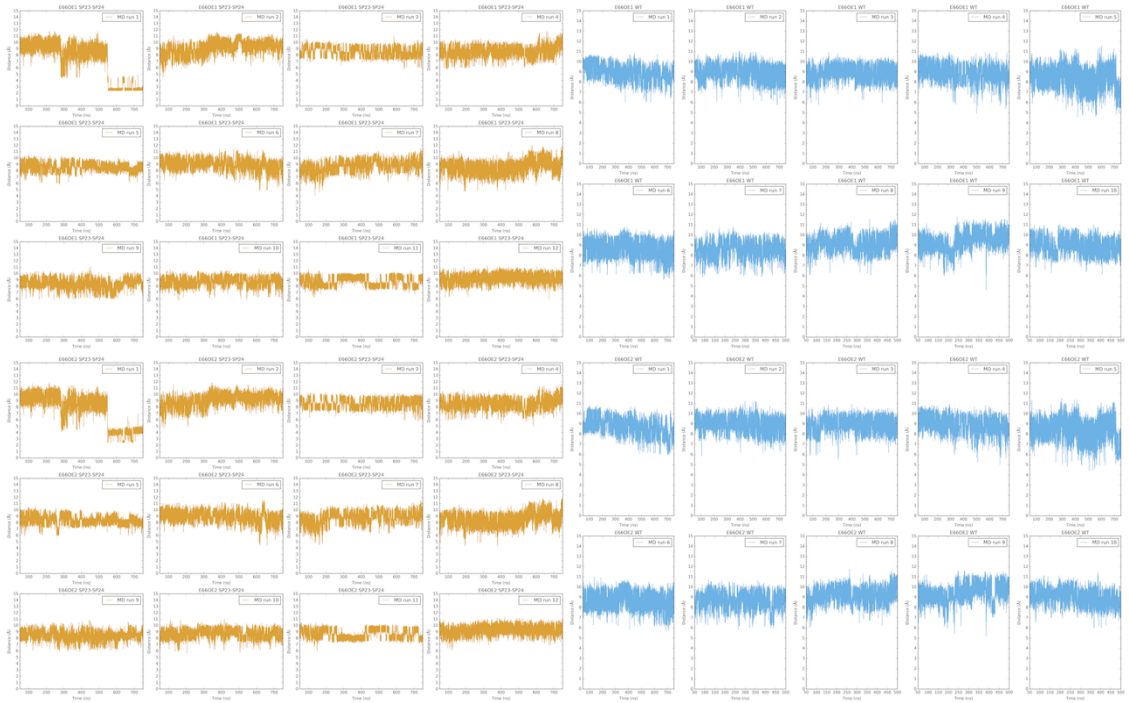

E76 OE1 and OE2

S69 OG

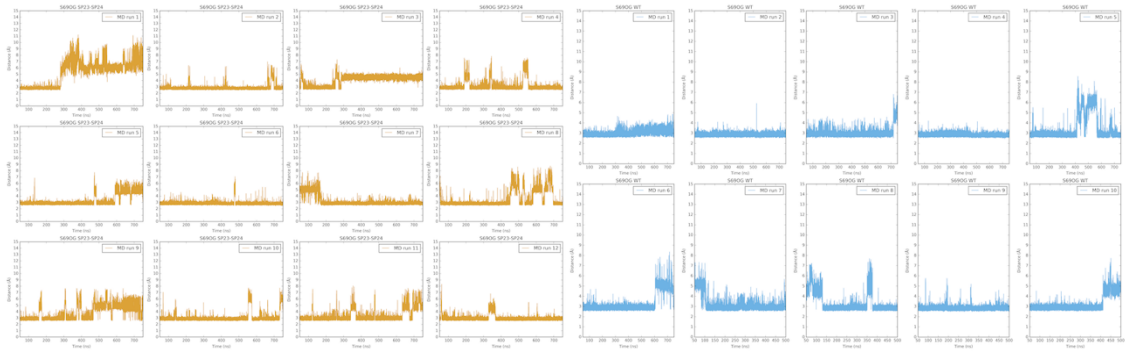

T71 O and OG1

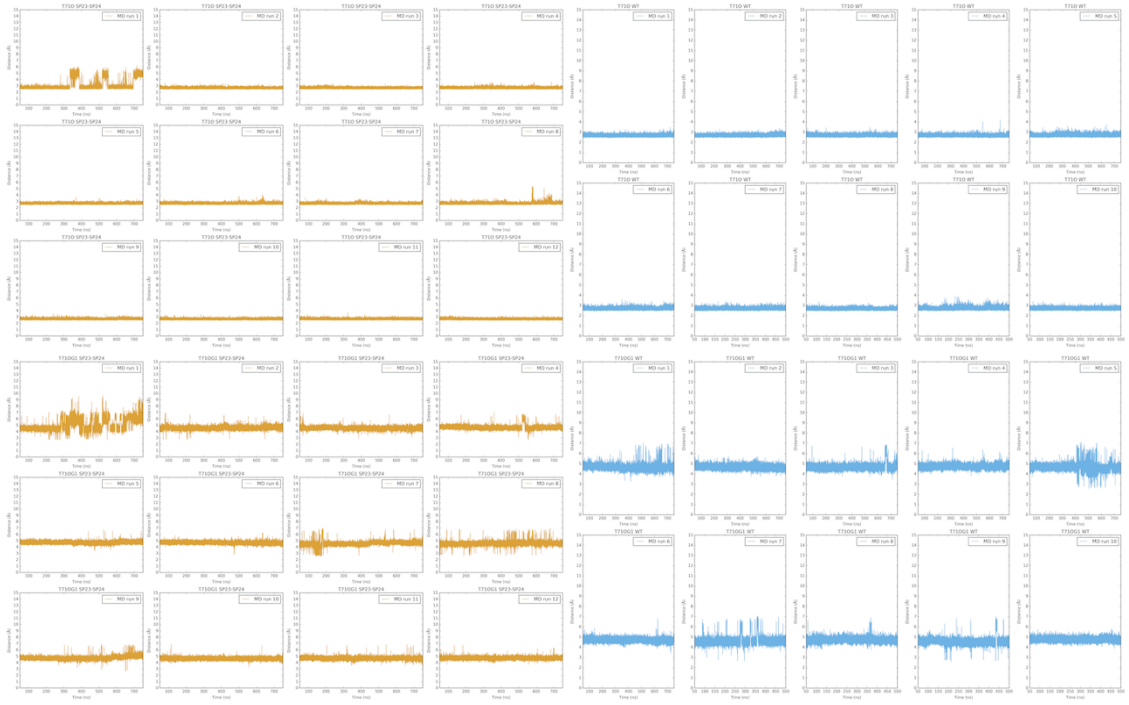

Figure S13. Time evolution of the distances between the catalytic Ca^{2+} and cTnC site II amino acids for each run. The WT systems are plotted in blue and the phosphorylated systems in orange.

Density comparisons

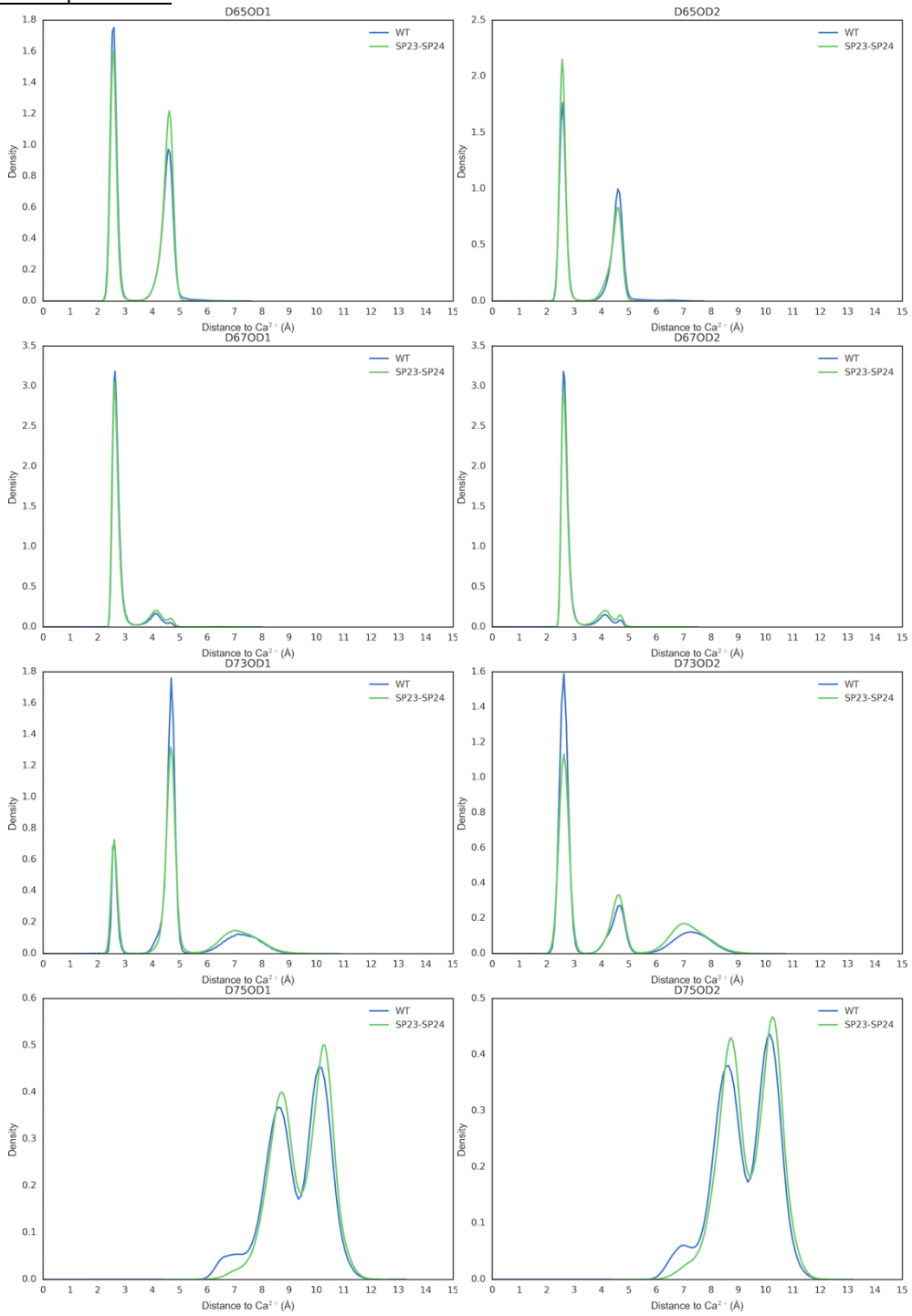

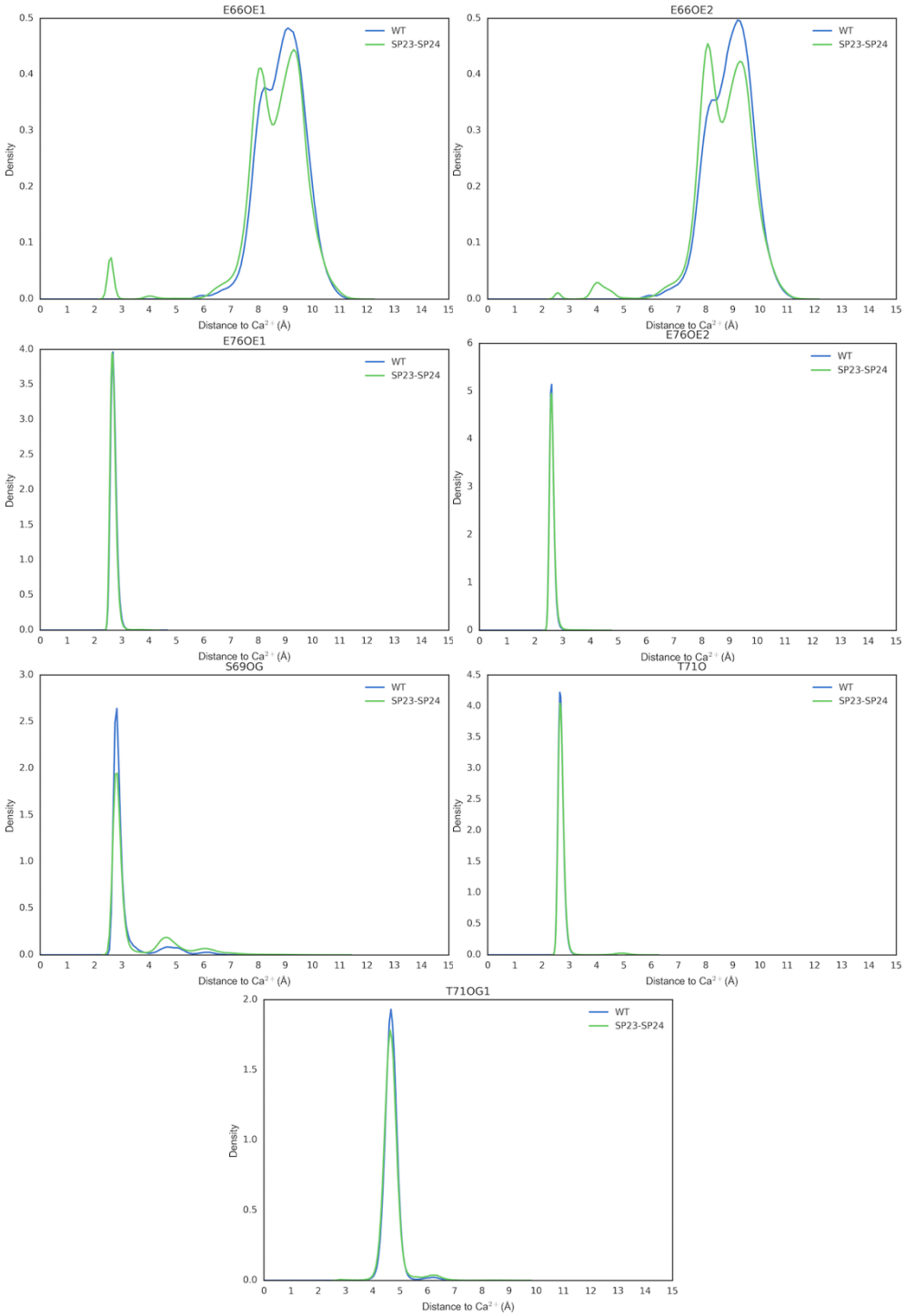

Figure S14. Comparison of the distance distributions between the WT and the SP23/SP24 systems for the aggregated time series of Figure S13.The distribution is smoothened with a Gaussian kernel density estimator.

Contact maps

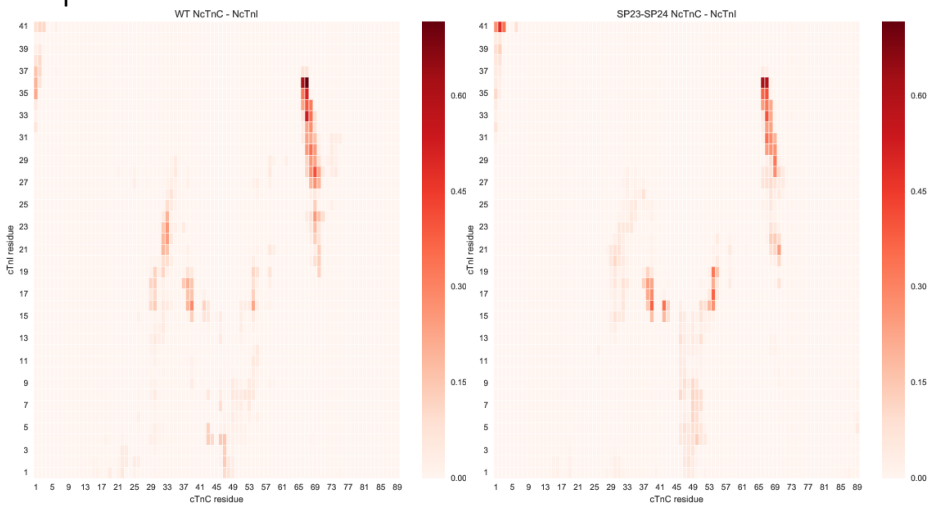

Figure S15. Average contact maps for the N-terminal cTnC (1-88) region against the N terminal cTnI region (1-41) in the unphosphorylated (WT) and phosphorylated (SP23/SP24 states).

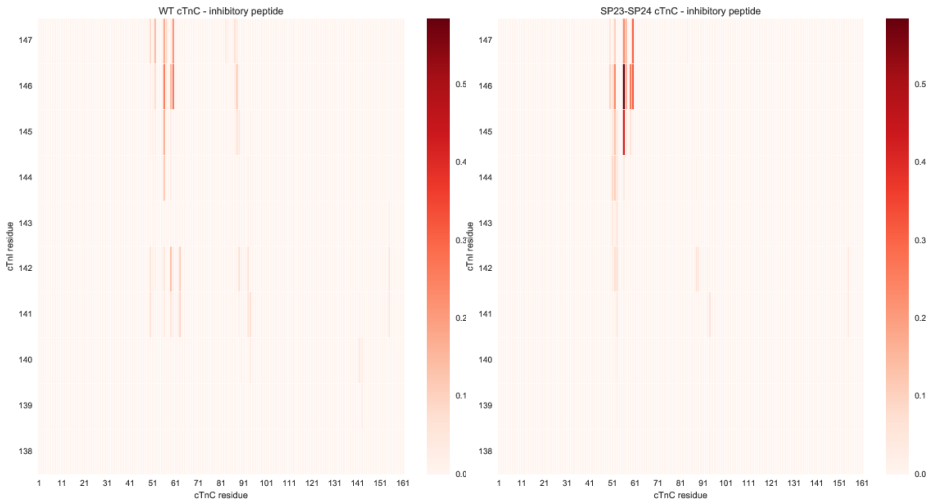

Figure S16. Average contact maps for the unphosphorylated (left), phosphorylated (right) systems between the complete cTnC molecule and the cTnI inhibitory peptide.

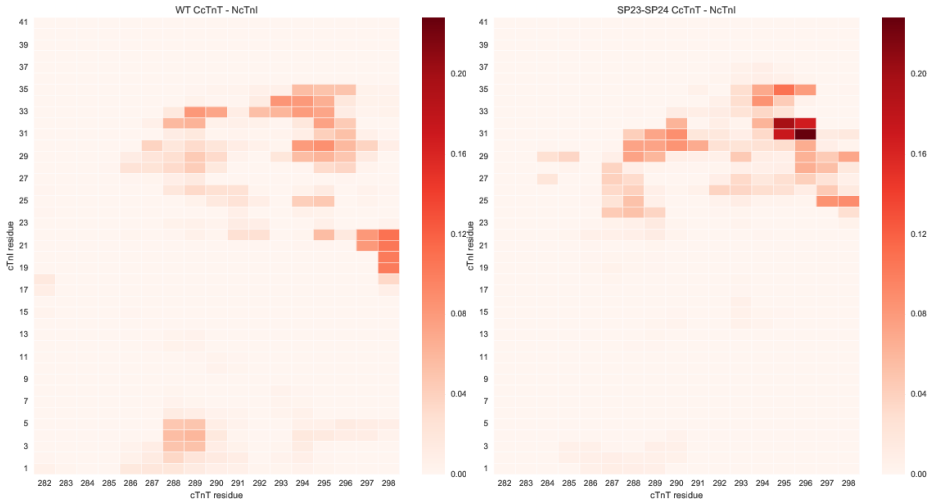

Figure S17. Average contact maps for the unphosphorylated (left) and phosphorylated (right) systems between the C terminal region of cTnT and the N terminal region of cTnI.

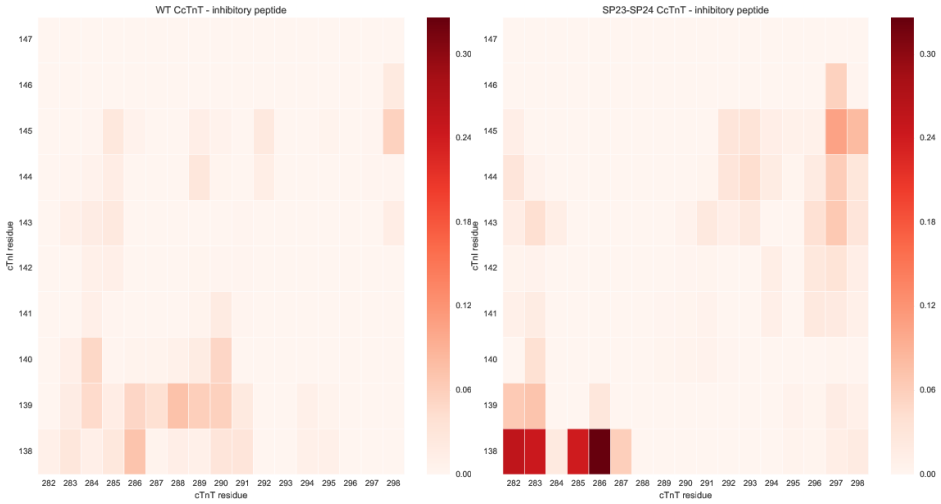

Figure S18. Average contact maps for the unphosphorylated (left) and phosphorylated (right) systems between the C terminal region of cTnT and the cTnI inhibitory peptide.

Difference contact maps

The following six difference contact maps highlight the changes in fraction of contact between the studied regions introduced by phosphorylation. The win/loss of contact values are mapped from the color bar, and the associated standard deviations are annotated as text in each cell. As can be observed, the standard deviation is always equal (or larger) than the absolute value of the difference.

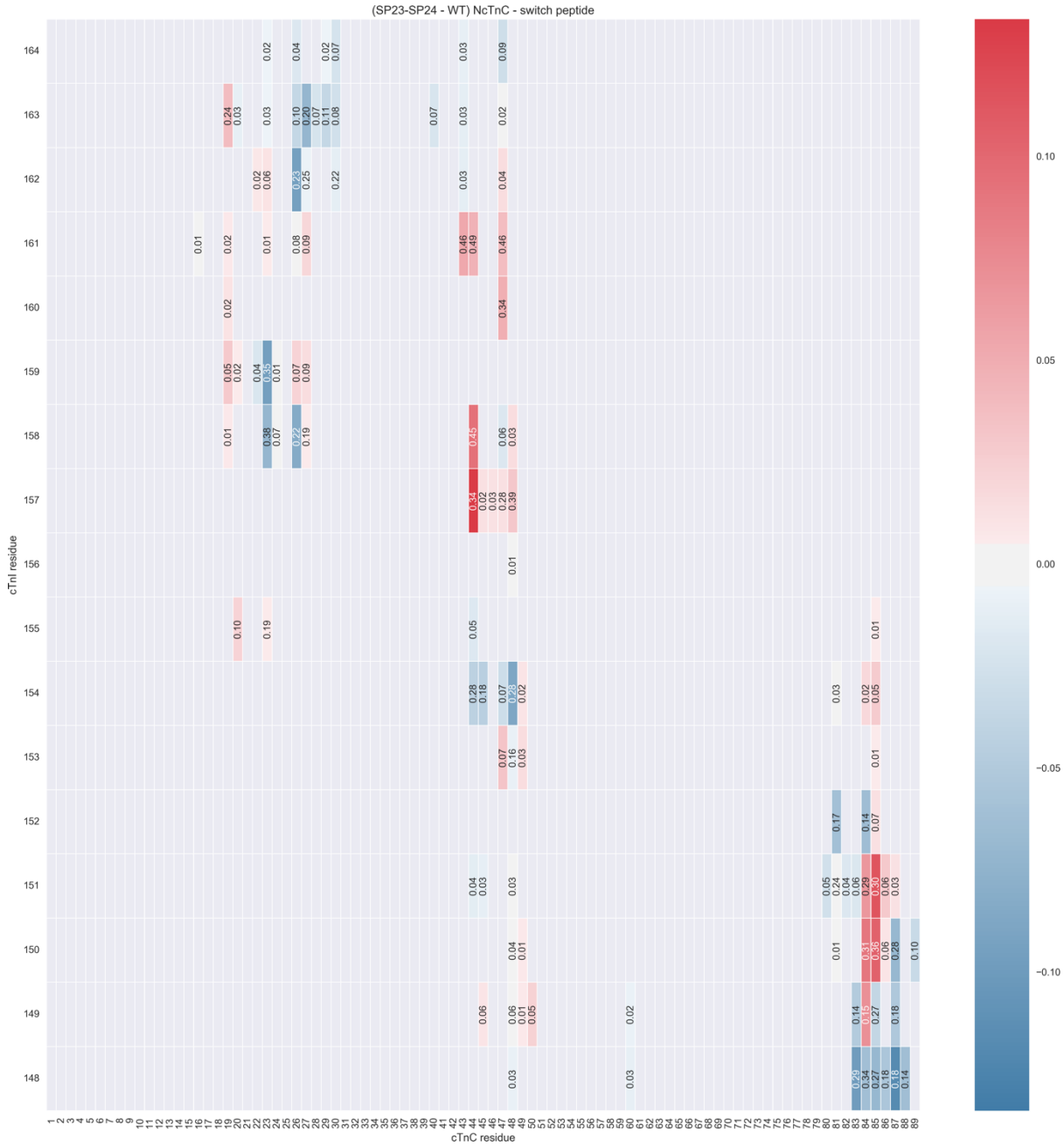

Figure S19. Difference contact map between the N-terminal region of cTnC and the switch peptide of cTnI.

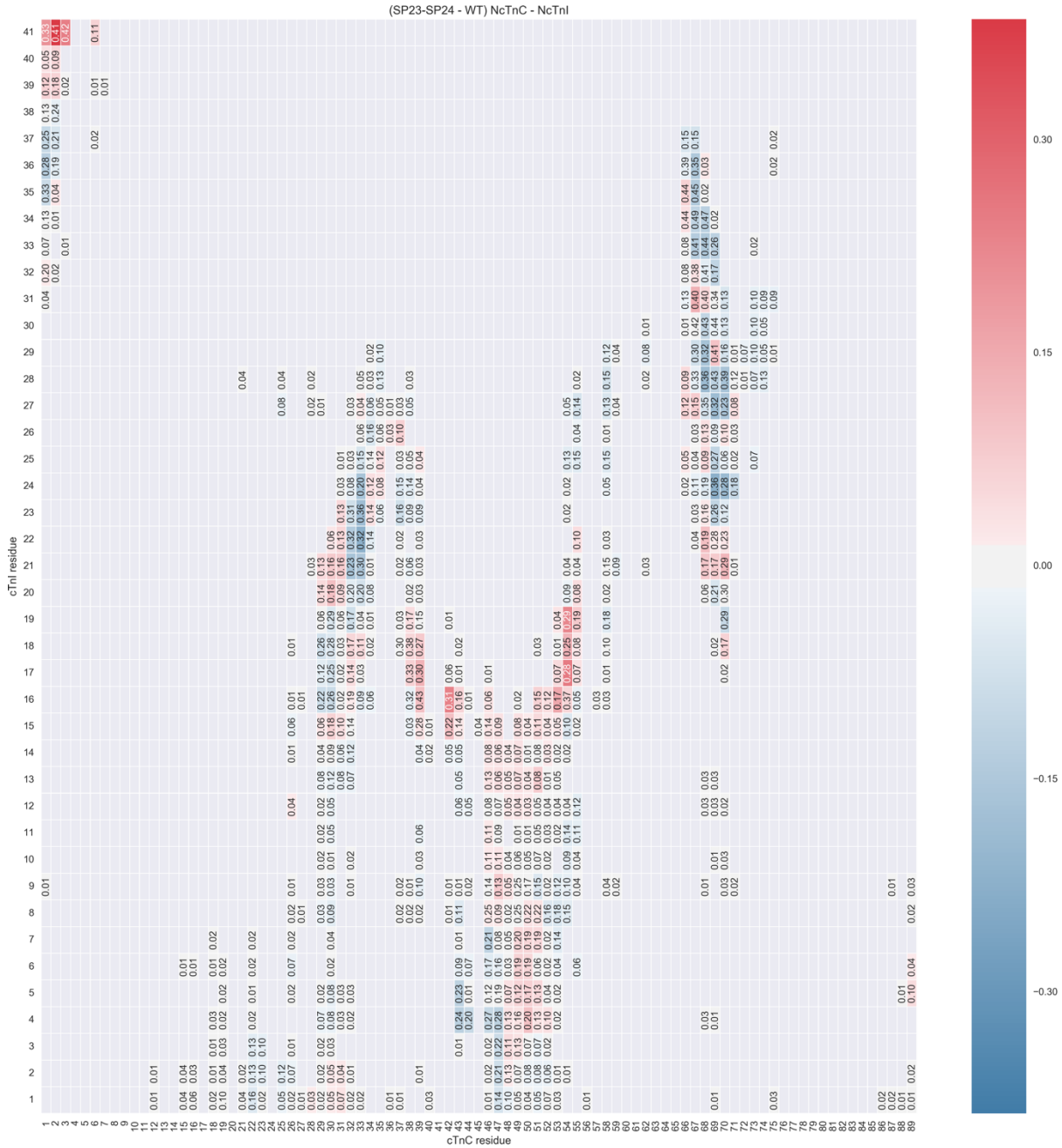

Figure S20. Difference contact map between the N- terminal region of cTnC and the N – terminal region of cTnI.

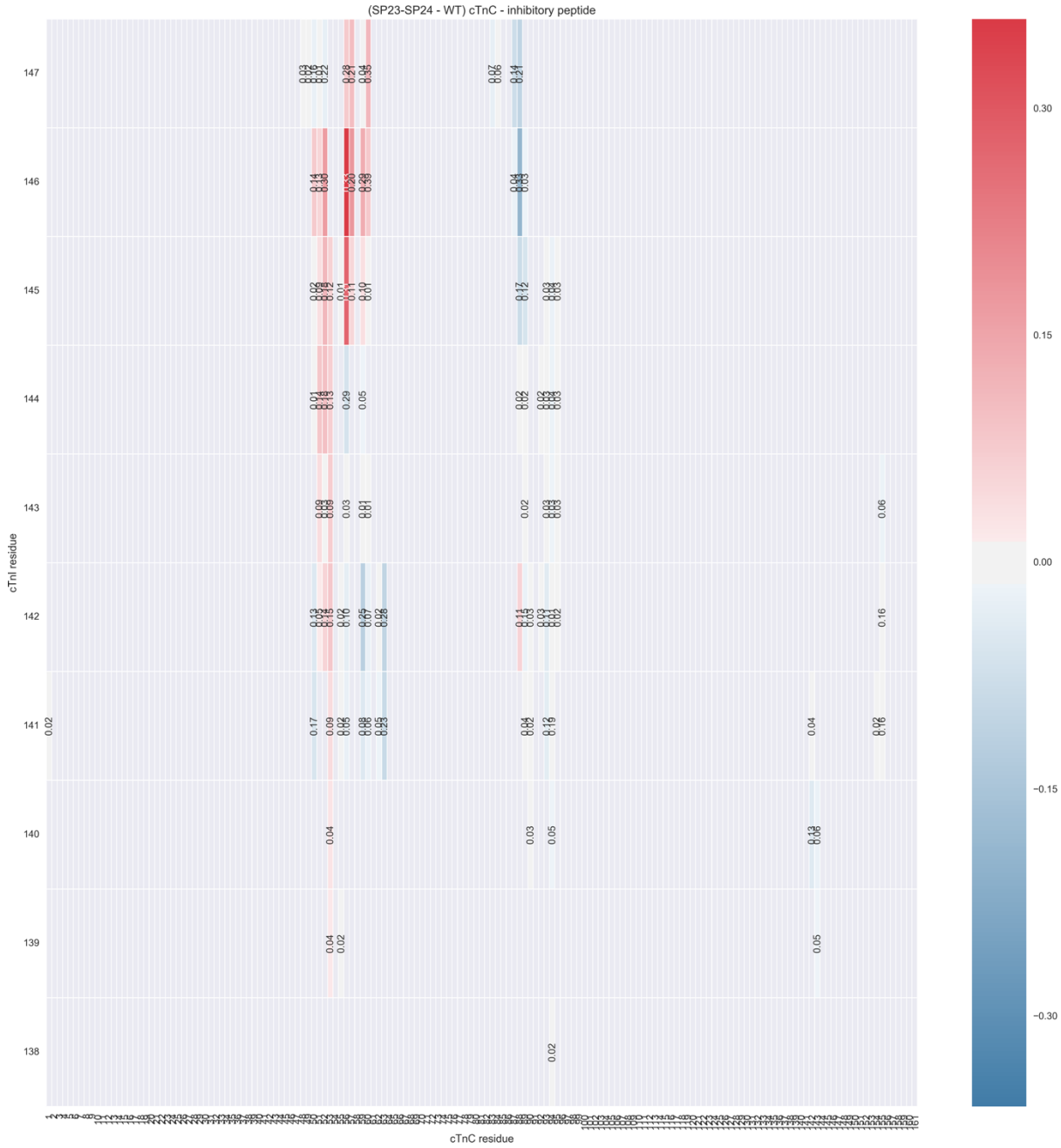

Figure S21. Difference contact map between the complete cTnC protein and the inhibitory peptide of cTnI.

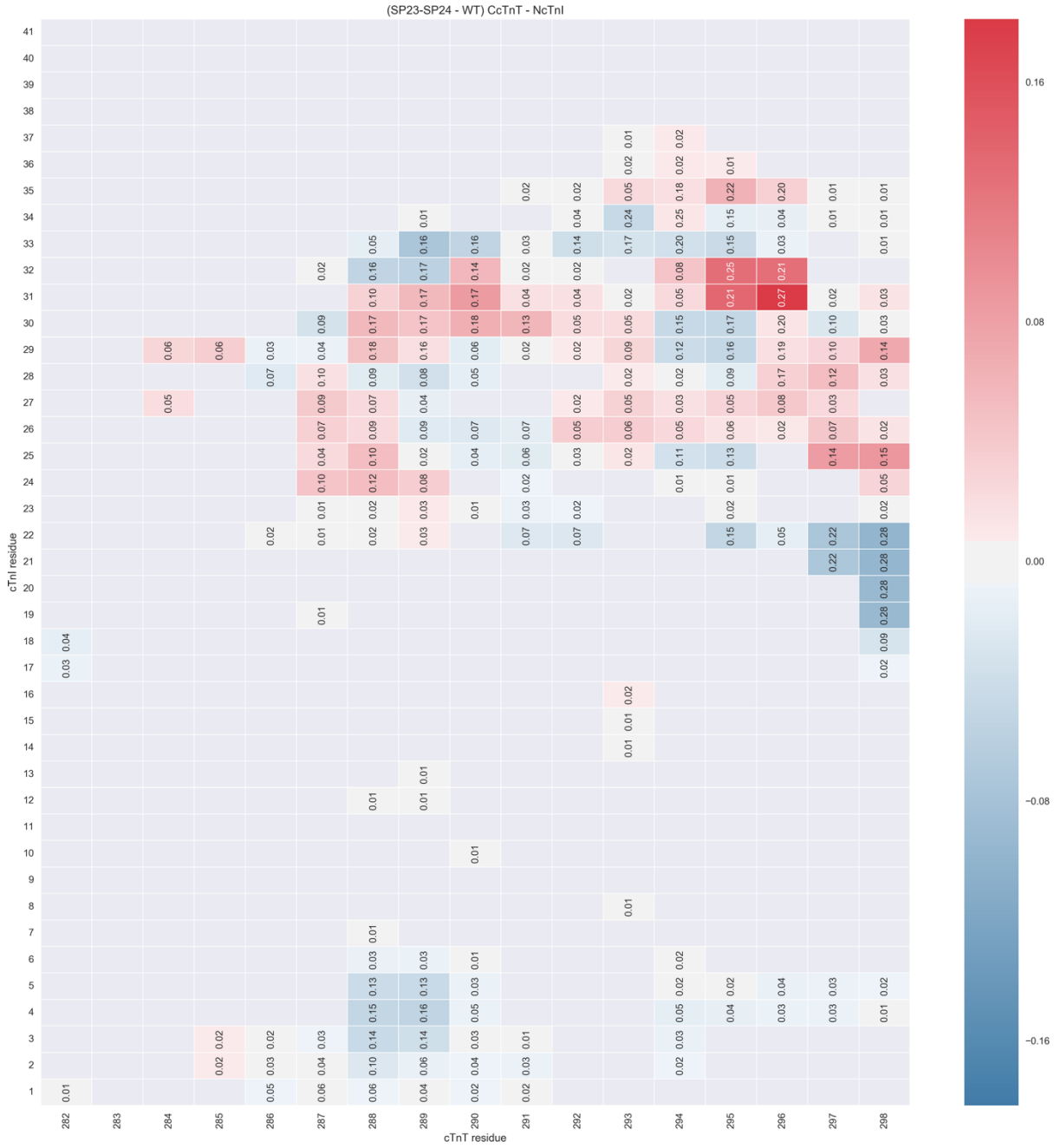

Figure S22. Difference contact map between the C terminal region of cTnT and the N-terminal region of cTnI.

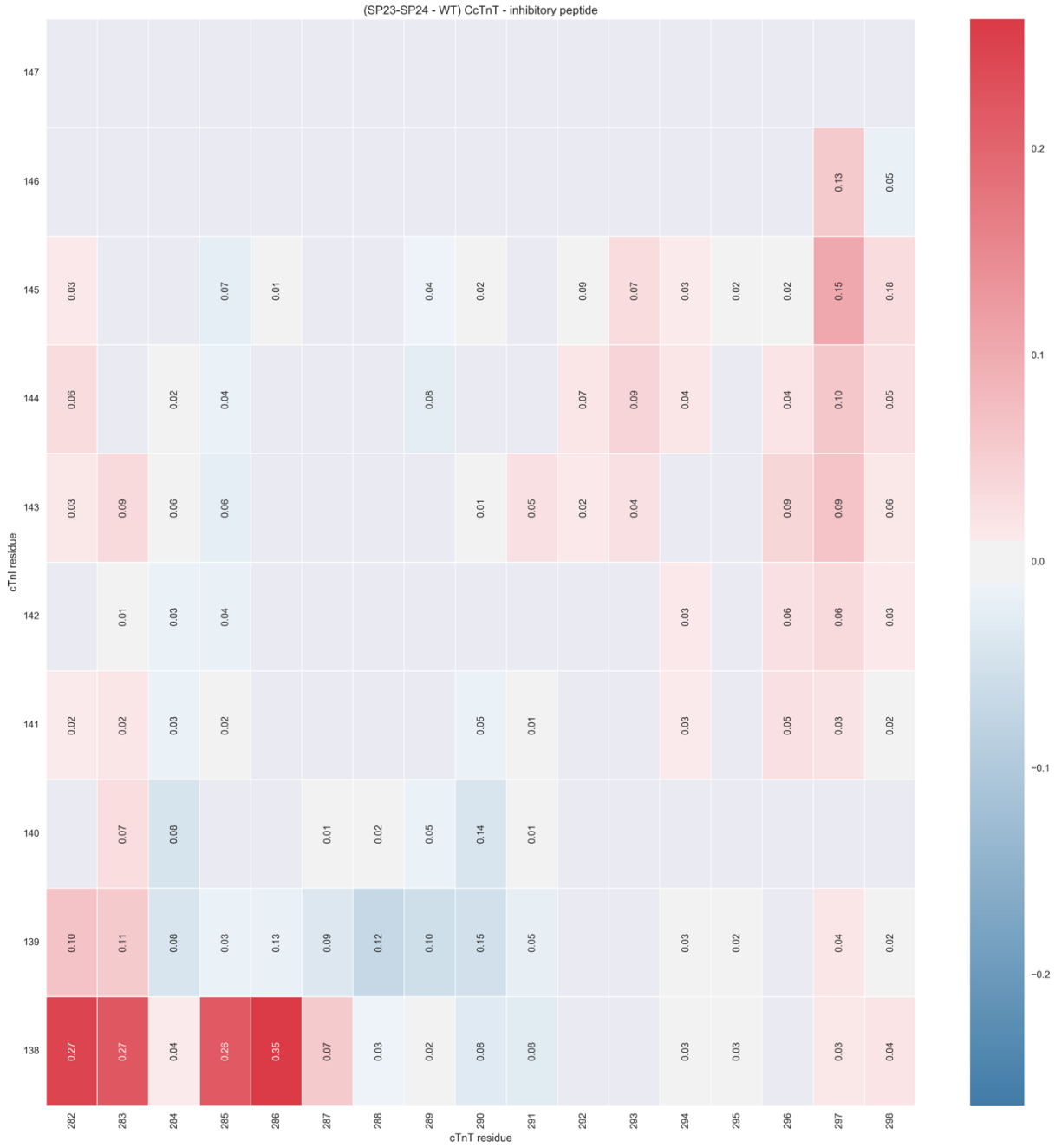

Figure S23. Difference contact map between the C terminal region of cTnT and the inhibitory peptide of cTnI.

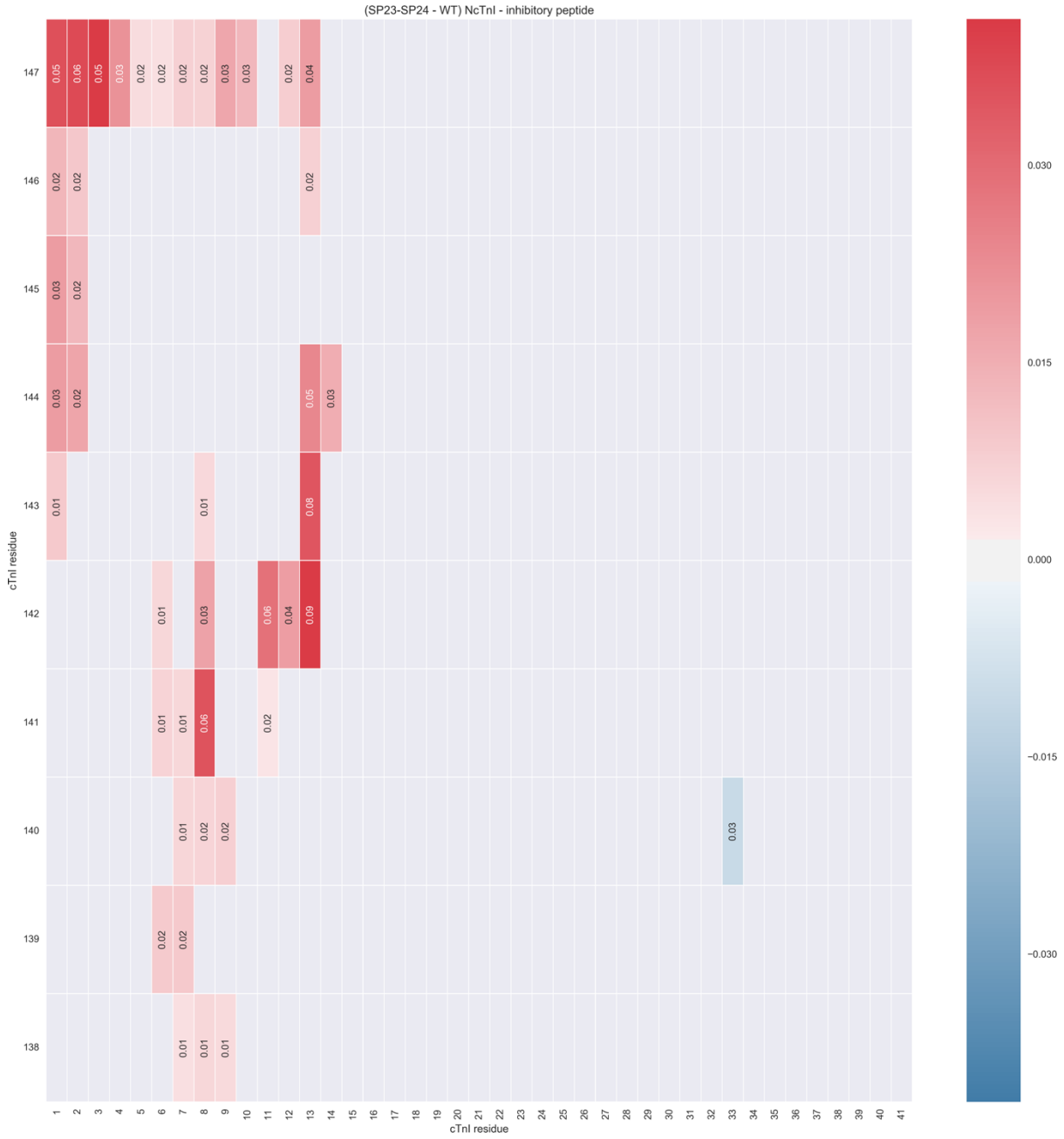

Figure S24. Difference contact map between the N-terminal region of cTnI and the inhibitory peptide of cTnI.